STATE RESEARCH CENTER OF RUSSIA
Institute of Theoretical
and Experimental Physics

28-96

V.L. Morgunov, I.O. Pilugin

Low-Energy Neutrino Weak and Electromagnetic Scattering Cross Sections on Atomic Electrons.

Moscow 1996

UDK 530.1 М-16

LOW ENERGY NEUTRINO WEAK AND ELECTROMAGNETIC SCATTERING CROSS SECTIONS ON THE ATOMIC ELECTRONS: Preprint ITEP 28-96/

V.L.Morgunov[1], I.O.Pilugin[2] - M., 1996 - 16p.

Neutrino scattering on atomic electrons due to weak and electromagnetic moment interactions is considered. We have found:

- nonzero cross section beyond the kinematical limit,
- logarithmic collinear divergence for electromagnetic cross-section,
- that electromagnetic cross section tends to a constant at $T \to 0$ instead of the $1/T$ behaviour,
- reduction of the total cross section in comparison with the free electron case scattering.

Fig. - 7, ref. - 15.

[1]E-mail : morgunov@vxitep.itep.ru
[2]E-mail : pilugin@vxitep.itep.ru

Introduction

The well-known deficit of Solar Neutrino Flux can be explained by supposing that neutrino has a small magnetic moment $\sim 10^{-10} - 10^{-11}\mu_B$ ([1] and literature afterwards). The value of μ_{ν_e} affects several astrophysical and cosmological phenomena such as white dwarf cooling [2] or red giant evolution [3]. The existence of the neutrino magnetic moment also implies a new physics beyond the Standard Model of Electro-Weak Interactions.

The interest to the direct measurements of the neutrino magnetic moment arose during the last decade. The modern design of the neutrino sources includes radioactive isotopes, such as ^{3} H, ^{55} Fe, ^{147} Pm [4] with low-energy neutrino spectrum. The neutrino energy of those sources is of the order of K-shell energies of the atoms Xe^{54} or I^{53}, which are considered in the neutrino detector proposals [5].

Measurements of the neutrino magnetic moment require an accurate knowledge of the differential neutrino cross section behavior but, the well-known approximation for the neutrino scattering on free electrons can lead to quite big errors in the cross section estimate for low-energy neutrino experiments. We could find only two papers on the subject ([6] and [7]) , both making different conclusions.

Weak interaction

Consider first the weak interaction of a neutrino. If $(\omega_1, \vec{k_1})$ and $(\omega_2, \vec{k_2})$ are the energy and momentum of the plane wave functions of the initial and final neutrino, $E_1 = m_e + E_{\tilde{n},\tilde{l}}$ is the energy the bound electron with $\tilde{n}, \tilde{l}$ quantum numbers ($E_{\tilde{n},\tilde{l}} < 0$), and ($E_2 = m_e + T,\ \vec{p}$) are the energy and momentum of a recoil electron moving in the selfconsistent atomic field, one can write the formulae for the weak neutrino cross section on the bounded electron as

$$d\sigma^W_{\tilde{n},\tilde{l}} = \sum_{\tilde{m}=\tilde{l}}^{\tilde{l}} \frac{\overline{|M_{fi}|^2}}{2\ \omega_1} 2\pi\delta(\ \omega_1 + E_1 -\ \omega_2 - E_2) \frac{d^3k_2}{(2\pi)^3 2\ \omega_2} \frac{d^3p}{(2\pi)^3}\ , \qquad (1)$$

and the differential cross section as

$$\frac{d\sigma^W_{\tilde{n},\tilde{l}}}{dT} = \sum_{\tilde{m}=\tilde{l}}^{\tilde{l}} \int \frac{2\overline{|M_{fi}|^2}}{(4\pi)^5} \frac{\omega_2}{\omega_1} m_e |\vec{p}| d\Omega_{k_2} d\Omega_p\ . \qquad (2)$$

Here we write in (1) the usual expression with the energy delta function, because the initial electron has a momentum distribution. The matrix element of the weak neutrino scattering with charged W^+ and neutral Z^0 currents is

$$M_{fi} = 2\sqrt{2}\, G_F \overline{U}_{k_1} \gamma_\alpha \frac{1}{2}(1+\gamma_5) U_{k_1}\, \overline{U}_2 \left[g_L \gamma^\alpha \frac{1}{2}(1+\gamma_5) + g_R \gamma^\alpha \frac{1}{2}(1-\gamma_5) \right] U_1 \ . \tag{3}$$

We use the bispinors $U_{1,2}$ of the electrons in the first order of v/c expansion, with the Hartree-Fock and Coulomb wave functions in the atomic field, respectively:

$$U_1 = \begin{pmatrix} w_1 \\ 0 \end{pmatrix} \psi_{\tilde{n},\tilde{l}}(\vec{r}) \quad ; \quad U_2 = \begin{pmatrix} w_2 \\ \frac{\vec{\sigma}\vec{p}}{E_2+m_e} w_2 \end{pmatrix} \psi_{\vec{p},l}(\vec{r}) \tag{4}$$

After summing and averaging of the polarizations we get

$$\overline{|M_{fi}|^2} = 64 G_F^2\, |J|^2 \left[g_L^2\, \omega_1 \left(\omega_2 - \frac{\vec{p}\vec{k}_2}{E_2} \right) + g_R^2\, \omega_2 \left(\omega_1 - \frac{\vec{p}\vec{k}_1}{E_2} \right) + g_L\, g_R\, \frac{q^2}{2} \right] , \tag{5}$$

where: $q = (q_0, \vec{q}) = k_1 - k_2$ and $J = J(\theta, \theta', \varphi')$ is an integral of the wave functions overlap (see Appendix 1). Factorizing the functions into the radial and spherical parts and integrating over r we obtain:

$$J(\theta, \theta', \varphi') = 4\pi \sum_{l_2} (-i)^{l_2} Y_{l_2 \tilde{m}}(\theta', \varphi') I_{l_2}(\theta) \tag{6}$$

where: θ', φ' are the spherical angles of $\vec{p}$ with respect to $\vec{q}$ and θ is the angle between $\vec{k}_1$ and $\vec{k}_2$. For definition of the function $I_{l_2}(\theta)$ see Appendix 1. Thus the final formula for the neutrino weak scattering differential cross section is

$$\frac{d\sigma^W_{\tilde{n},\tilde{l}}}{dT} = \sum_{\tilde{m}=\tilde{l}}^{\tilde{l}} \frac{2G_F^2 m_e}{\pi} \frac{1}{\omega_1^2} \int d\cos\theta \left[\left(g_L^2\, \omega_1\, \omega_2 + g_R^2\, \omega_1\, \omega_2 + g_L g_R \frac{q^2}{2} \right) S_0^{\tilde{n},\tilde{l}} - \right.$$

$$\left. - \left(g_L^2\, \omega_1 \frac{\vec{q}\vec{k}_1}{q E_2} + g_R^2\, \omega_2 \frac{\vec{q}\vec{k}_2}{q E_2} \right) |\vec{p}| S_1^{\tilde{n},\tilde{l}} \right] , \tag{7}$$

where:

$$S_0^{\tilde{n},\tilde{l}}(\theta) = \frac{2}{\pi}\, \omega_1\, \omega_2 |\vec{p}| \sum_{l_2} |I_{l_2}|^2 \ ;$$

$$S_1^{\tilde{n},\tilde{l}}(\theta) = \frac{2}{\pi\sqrt{3}}\,\omega_1\,\omega_2|\vec{p}|\sum_{l_2}\left[W_+ I_{l_2} I_{l_2+1} - W_- I_{l_2} I_{l_2-1}\right] \ , \qquad (8)$$

are the dimensionless functions (shown in Fig. 1) and W_i are Wigner-like coefficients (see Appendix 2). The value of the cross section of the antineutrino scattering is derived by the substitution $g_R \leftrightarrow g_L$.

Equation (7) tends asymptotically to the free electron case, if we take into account that $S_1^{\tilde{n},\tilde{l}} \to S_0^{\tilde{n},\tilde{l}}$, because $W_+ \sim -W_- \to \sqrt{3}/2$ and I_{l_2} is the smooth function of the l_2 , and that the distribution function $S_0^{\tilde{n},\tilde{l}}(\theta)$ of the neutrino scattering angle with the fixed recoil electron energy is the δ-function of θ: $\delta(cos(\theta) - cos(\theta_{|\vec{q}|=|\vec{p}|}))$. The illustration of such transition of $S_0^{\tilde{n},\tilde{l}}(\theta)$ is shown in the Fig. 1. The maximum of this function corresponds to $cos\theta_{|\vec{q}|=|\vec{p}|}$, i.e. momentum conservation.

Similar distribution functions were observed in the Compton scattering measurements [8], where the distribution of the atomic electron momentum leads to the spread of the photon energy at fixed scattering angle. Such measurements were used for the reconstruction of the electron wave functions inside atoms.

If we substitute the previously mentioned angular delta-function instead of $S_0^{\tilde{n},\tilde{l}}$ and $S_1^{\tilde{n},\tilde{l}}$, we can get the well known formulae of the cross section for the free electron-neutrino scattering [9, 10]:

$$\frac{d\sigma^W_{\nu e}}{dT} = \frac{2G_F^2 m_e}{\pi}\left[g_L^2 + g_R^2\left(1 - \frac{T}{\omega_1}\right)^2 - g_L\, g_R\,\frac{m_e T}{\omega_1^2}\right] \ ;$$

$$\frac{d\sigma^W_{\overline{\nu} e}}{dT} = \frac{d\sigma^W_{\nu e}}{dT}(g_R \leftrightarrow g_L) \qquad (9)$$

Electromagnetic interaction

We can write the electromagnetic neutrino scattering matrix element as

$$M_{fi} = \mu_{\nu_e}\frac{e}{2m_e}(\overline{U}^R_{k_2}\sigma_{\mu\nu}q_\nu U^L_{k_1})\,\frac{g_{\mu\lambda}}{q^2}\,(\overline{U_2}\,ie\gamma_\lambda\,U_1) \qquad (10)$$

where:

$$\overline{U}^R_{k_2} = U^+_{k_2}\gamma_0\frac{1}{2}(1+\gamma_5) \ ; \ U^L_{k_1} = \frac{1}{2}(1+\gamma_5)U_{k_1} \qquad (11)$$

and the magnetic moment μ_{ν_e} is in Bohr magnetons.

There is no interference of the electromagnetic and weak interactions, because of the different final states – in the first case the scattered neutrino is left-handed, and in the second one it is right-handed.

After summing and averaging of polarizations we have:

$$\sum_{\sigma_1\sigma_2} |M_{fi}|^2 = \mu^2_{\nu_e}\frac{e^4}{m_e^2 q^2}(2m_e(\,\omega_1+\,\omega_2)[(\,\omega_1+\,\omega_2)E_2-(\vec{k_1}+\vec{k_2})\vec{p}]+q^2 m_e T))|J|^2 \,, \tag{12}$$

where function J is defined in Eq. 6. The procedure, which is similar to the previous section allows as to write the final formula for the electromagnetic scattering as:

$$\frac{d\sigma^{EM}_{\tilde{n},\tilde{l}}}{dT} = \mu^2_{\nu_e} \sum_{\tilde{m}=-\tilde{l}}^{\tilde{l}} \frac{\alpha^2\pi}{m_e^2} \int_{-1}^{1} \frac{F^{\tilde{n},\tilde{l}}(cos\theta)dcos\theta}{1-cos\theta} \,, \tag{13}$$

where $F^{\tilde{n},\tilde{l}}(cos\theta)$ is the regular function of θ at $\theta \to 0$:

$$\begin{aligned} F^{\tilde{n},\tilde{l}}(cos\theta) \;=\; & \frac{1}{4\,\omega_1\,\omega_2}\left\{\left[\left(1+\frac{\omega_2}{\omega_1}\right)^2 E_2 - \frac{\omega_2 T}{\omega_1}(1-cos\theta)\right] S_0^{\tilde{n},\tilde{l}} - \right. \\ & \left. \left[\frac{|\vec{p}|(\,\omega_1+\,\omega_2)}{|\vec{q}|}\left(1-\frac{\omega_2^2}{\omega_1^2}\right)\right] S_1^{\tilde{n},\tilde{l}}\right\} \end{aligned} \tag{14}$$

An asymptotic transition to the free case can be made by the replacement of $S_0^{\tilde{n},\tilde{l}}$ and $S_1^{\tilde{n},\tilde{l}}$ by $\delta(cos(\theta) - cos(\theta_{|\vec{q}|=|\vec{p}|}))$ that will lead to [9, 10]:

$$\frac{d\sigma^{EM}_{\nu e}}{dT} = \mu^2_{\nu_e}\frac{\alpha^2\pi}{m_e^2}\left(\frac{1}{T}-\frac{1}{\omega_1}\right) \tag{15}$$

Numerical results and discussion

Our method of calculations has been checked by the photoeffect cross section calculations for different atoms H, He, Ne, Xe [11]. In that article we considered the influence of the electron binding effect on the cross section, and we compare it with the experimental data. The agreement is good for $0.7 - 20keV$ of photon energy range, but for some shells the difference is about 50%, that can be explained by invalid Hartree-Fock functions.

All the peculiarities of the behavior of the neutrino weak and electromagnetic cross sections follow from the binding of the initial electron. It leads to the collinear divergence of an integral of $cos(\theta)$ (θ is the scattering angle) for the electromagnetic cross section Eq. 14. This divergence is logarithmic and it is restricted by the neutrino mass. The integrands from Eq. 14 are shown in Fig. 2, where the left peak is at $cos\theta_{|\vec{q}|=|\vec{p}_2|}$ i.e. at θ value dictated by the momentum conservation law and the right peak at the $cos\theta \to 1$ is the divergence we are discussing.

The second consequence is the nonzero cross section beyond the kinematic limit:

$$T_{max} = \frac{2\ \omega_1^2}{m_e + 2\ \omega_1}. \tag{16}$$

This phenomenon occurs for both weak and electromagnetic cross sections. Resultant curves of the differential cross sections of the antineutrino ($\omega_1 = 100keV$) weak and electromagnetic scattering on the atomic electrons are represented at Figs. 3,4, where we can see the influence of the binding effect: the less the shell energy the sharper edge of the electron kinetic energy spectrum.

The third influence is the reduction of the cross sections of the neutrino scattering by a factor whose value is the larger the larger the binding energy.

The differential cross sections $d\sigma_{\bar{\nu}e}^{EM}/dT$, $d\sigma_{\bar{\nu}e}^{W,Z}/dT$ for Xe^{54} atom summarized for all the shells and normalized on one electron are presented in Fig. 5 together with the cross sections calculated for the free electron. The differential cross sections for a few neutrino energies are shown in Fig. 6.

The reduction of the total weak cross section (integrated from T_{min} = 0.5 keV to $T_{max} = 100$ keV), as compared to the free electron cross section, after averaging over the Pm-neutrino spectrum (E_{min} = 0 keV, E_{max} = 220 keV) is about 9% and $\sigma_{Xe}^{W} = 54 \times 292. \times 10^{-24}$ $barn$; $\sigma_{free}^{W} = 324. \times 10^{-24}$ $barn$. For the electromagnetic cross section this difference exceed 15% and $\sigma_{Xe}^{EM} = 54 \times 93. \times 10^{-24}$ $barn$; $\sigma_{free}^{EM} = 109. \times 10^{-24}$ $barn$. The reason of the stronger reduction of the electromagnetic cross section is that the main part of the total cross section comes from small T, but the binding cuts the divergence of $1/T$ and it tends to the constant. So, a binding of any kind cuts of the divergence. Besides this $1/T$ divergence we have the weak logarithmic divergence of $cos\theta$ Eq. 14, but it is unessential.

Thus we qualitatively confirm the results presented by Fayans et al. [6], where they used in calculations the relativistic wave functions for Mo^{42} and F^9 atomic electrons, and we disagree with the statement in the article [7] about the increase of the cross sections.

In the Fig. 7 we show the dependence of the ratio of the electromagnetic ($\mu_\nu = 10^{-11}\mu_B$) and weak total cross sections on neutrino energy. So one can see that low neutrino energies are more preferable for the neutrino magnetic moment measurements.

The authors are grateful to K.A. Ter-Martirosyan and L.B. Okun for encouraging discussions and to B.V. Geshkenbein and D.V. Chekin for the valid comments.

Appendix 1

$$J = \int \psi^*_{\vec{p}_2 l_2}(\vec{r})\, e^{i\vec{q}\vec{r}} \psi_{\tilde{n}\tilde{l}\tilde{m}}(\vec{r})\, d^3r \quad . \tag{17}$$

J can be represented as a product of two factors, because the wave functions factorize into radial and spherical parts. The function

$$\psi_{\tilde{n}\tilde{l}\tilde{m}}(\vec{r}) = R_{\tilde{n}\tilde{l}}(r) Y_{\tilde{l}\tilde{m}}(\Theta, \varphi) = Y_{\tilde{l}\tilde{m}}(\Theta, \varphi) \sum_j c_{l,j} N_j r^{n_j - 1} \exp\left(-\zeta_j r\right)$$

is the Hartree-Fock wave function of a bound electron with quantum numbers $\tilde{n}\tilde{l}\tilde{m}$ [12]. The wave function of the outgoing electron in atomic field is:

$$\psi_{\vec{p},l}(\vec{r}) = R_{\vec{p}_2 l_2}(r)(2l+1) P_l(\Theta_{\vec{p}\vec{r}}) \ , \tag{18}$$

where P_l is the Legendre polynomial. The $R_{\vec{p}_2 l_2}$ is the solution of the Shrödinger equation in an effective self-consistent potential inside the atom:

$$R_{p,l_2}(r) = \chi(r)/r \ ;$$

$$\frac{d^2\chi}{dr^2} + \left[T - 2m_e U(r) - \frac{l_2(l_2+1)}{r^2}\right]\chi = 0 \ ; \ \chi(0) = 0 \ ; \ \chi(\infty) = sin(pr + \delta_{l_2}) \tag{19}$$

where δ_{l_2} is the phase of the wave, which is not necessary in our consideration, since we are interested not in the asymptotic behaviour at $r \to \infty$, but in the values of the function at the atomic size, which define the dynamics of the interaction. The atomic potential $U(r)$ is given by the Hartfee-Fock wave functions :

$$U(r) = \frac{-Ze^2}{r} + e^2 \int_0^\infty \frac{n(r')d^3r'}{|\vec{r} - \vec{r'}|} \tag{20}$$

where:

$$n(r) = \frac{1}{4\pi} \left\{ \sum_{n,l,m,\sigma} R^2_{n,l}(r) - R^2_{\tilde{n},\tilde{l}}(r) \right\}$$

is the electron density that comes from the Hartree-Fock wave functions without the contribution of the recoil electron. Discussion on the accuracy of the Hartree-Fock electron functions can be found in [13, 14]. Using the Y_{lm} orthonormalization we can get:

$$J = 4\pi \sum_{l_2} Y_{l_2\tilde{m}}(\theta'\varphi')\ (-i)^{l_2} I_{l_2}(\theta)\ , \tag{21}$$

where:

$$I_{l_2} = \sum_{l_1=|l_2-\tilde{l}|}^{l_2+\tilde{l}} \sqrt{2l_1+1} J_{rad}(l_1)(-1)^{l_1} \begin{pmatrix} l_2 & l & l_1 \\ -\tilde{m} & \tilde{m} & 0 \end{pmatrix} \tag{22}$$

with

$$J_{rad}(l_1) = \int_0^\infty R_{p,l_2}(r)\ j_{l_1}(|\vec{q}|r)\ R_{\tilde{n}\tilde{l}}(r) r^2 dr, \tag{23}$$

where $j_l(x)$ is the spherical Bessel function.

Appendix 2

The product of two spherical functions is a new function of θ and φ which can be decomposed over the spherical functions basis, i.e. according to the momentum sum rule:

$$Y_{l_1m_1} Y_{l_2m_2} = \frac{1}{\sqrt{4\pi}} \sum_{l=|l_1-l_2|}^{l_1+l_2} \begin{pmatrix} l_1 & l_2 & l \\ m_1 & m_2 & m \end{pmatrix} Y_{lm}\ , \tag{24}$$

where $m = m_1 + m_2$, because the projection on the z-axis must be conserved. So,

$$\begin{pmatrix} l_1 & l_2 & l \\ m_1 & m_2 & m \end{pmatrix} = \sqrt{4\pi} \int Y_{l_1 m_1} Y_{l_2 m_2} Y^*_{lm} d\Omega \tag{25}$$

Normalization $1/\sqrt{4\pi}$ is convenient to avoid π in all formulae. Using the formulae from [15] we write:

$$\int Y_{l_1 m_1} Y_{l_2 m_2} Y^*_{lm} d\Omega = (-1)^m \, i^{l_1+l_2-l} \begin{pmatrix} l & l_1 & l_2 \\ -m & m_1 & m_2 \end{pmatrix}_L \times$$

$$\times \begin{pmatrix} l & l_1 & l_2 \\ 0 & 0 & 0 \end{pmatrix}_L \left[\frac{(2l+1)(2l_1+1)(2l_2+1)}{4\pi} \right]^{1/2} , \tag{26}$$

where:

$$\begin{pmatrix} j_1 & j_2 & j_3 \\ m_1 & m_2 & m_3 \end{pmatrix}_L = \left[\frac{(j_1+j_2-j_3)!(j_1-j_2+j_3)!(-j_1+j_2+j_3)!}{(j_1+j_2+j_3+1)!} \right]^{1/2} \times$$

$$\times \left[(j_1+m_1)!(j_1-m_1)!(j_2+m_2)!(j_2-m_2)!(j_3+m_3)!(j_3-m_3)! \right]^{1/2} \times$$

$$\times \sum_z \left[\frac{(-1)^{z+j_1-j_2-m_3}}{z!(j_1+j_2-j_3-z)!(j_1-m_1-z)!(j_2+m_2-z)!} \times \right.$$

$$\left. \times \frac{1}{(j_3-j_2+m_1+z)!(j_3-j_1-m_2+z)!} \right] \tag{27}$$

In the text we use the following notation for $W_\pm$:

$$W_\pm = \begin{pmatrix} 1 & l_2 & l_2 \pm 1 \\ 0 & \tilde{m} & \tilde{m} \end{pmatrix} \tag{28}$$

The function $S_o(\cos\theta)$ (Eq. 8)

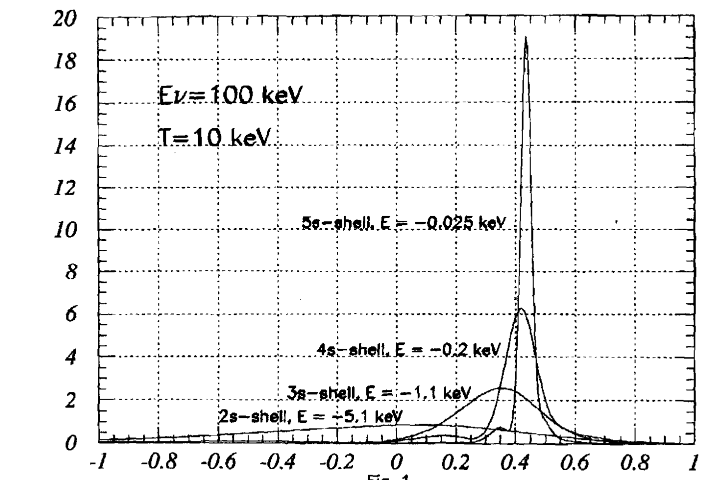

Fig. 1

The function $F(\cos(\theta))/(1-\cos(\theta))$ (Eq. 14)

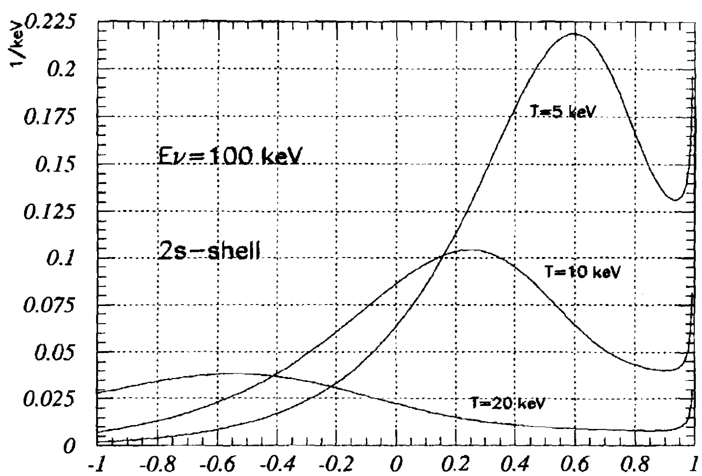

Fig. 2

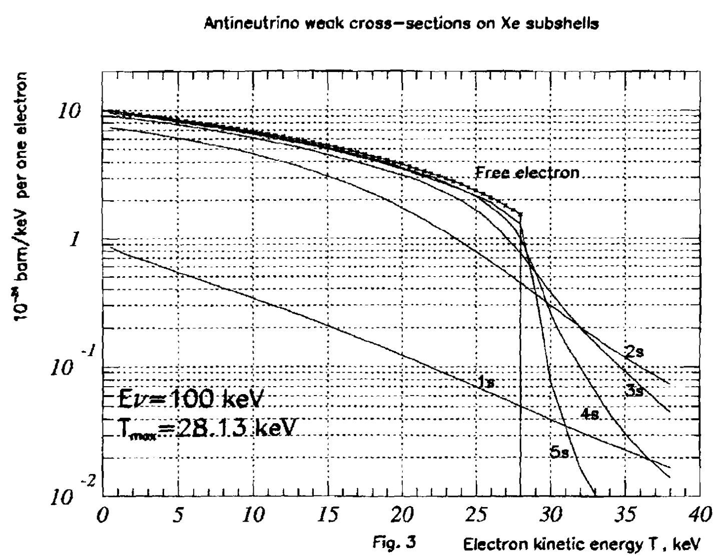

Antineutrino weak cross-sections on Xe subshells
10^{-46} barn/keV per one electron
10
1
10^{-1}
10^{-2}
0
5
10
15
20
25
30
35
40
Free electron
2s
3s
1s
4s
5s
$E\nu$=100 keV
T_{max}=28.13 keV
Electron kinetic energy T, keV

Fig. 3

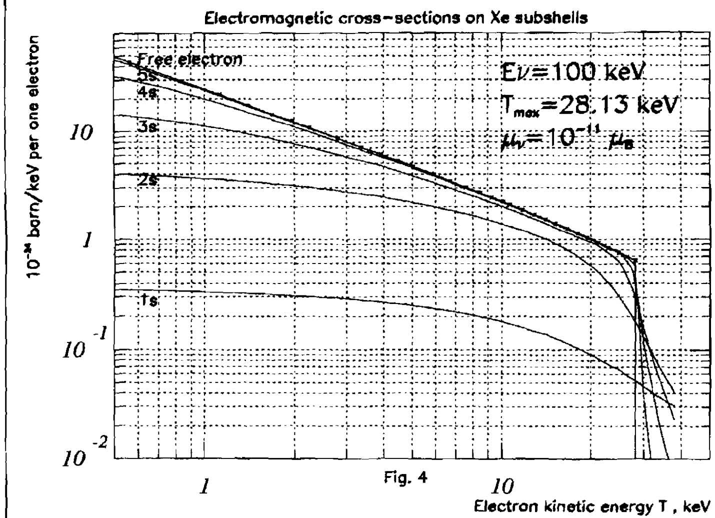

Electromagnetic cross-sections on Xe subshells
10^{-24} barn/keV per one electron
Free electron
5s
4s
3s
2s
1s
$E\nu$=100 keV
T_{max}=28.13 keV
μ_ν=10^{-11} μ_B
10
1
10^{-1}
10^{-2}
1
10
Electron kinetic energy T , keV

Fig. 4

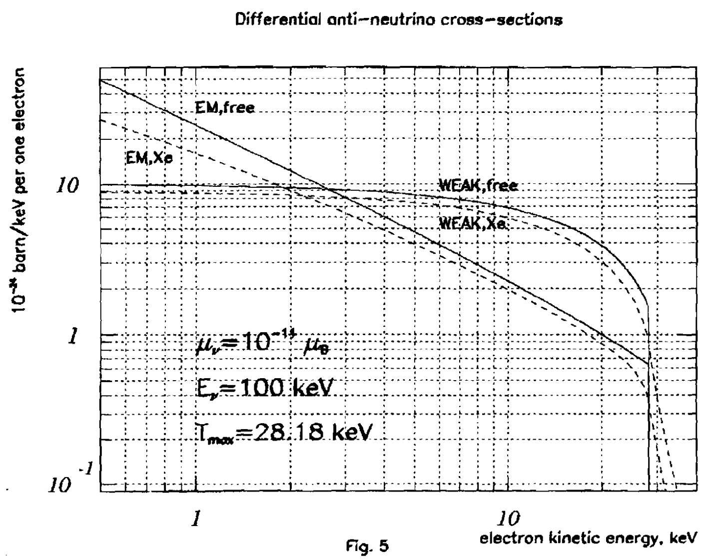
Differential anti-neutrino cross-sections
10^{-46} barn/keV per one electron
EM,free
EM,Xe
WEAK,free
WEAK,Xe
$\mu_\nu = 10^{-11}\ \mu_B$
$E_\nu = 100$ keV
$T_{max} = 28.18$ keV
10
1
10^{-1}
1
10
electron kinetic energy, keV
Fig. 5

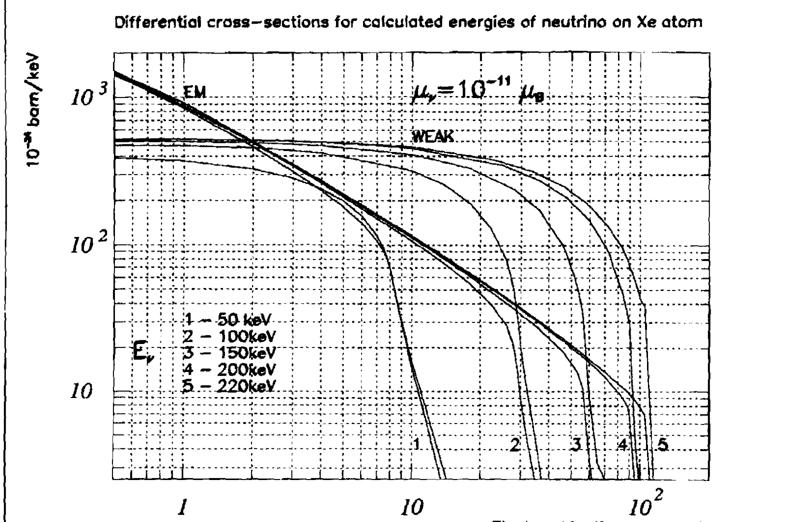
Differential cross-sections for calculated energies of neutrino on Xe atom
10 barn/keV
EM
WEAK
$\mu_\nu = 10^{-11}\ \mu_B$
E_ν
1 - 50 keV
2 - 100keV
3 - 150keV
4 - 200keV
5 - 220keV
1
10
10^2
10^3
Electron kinetic energy, keV

Fig. 6

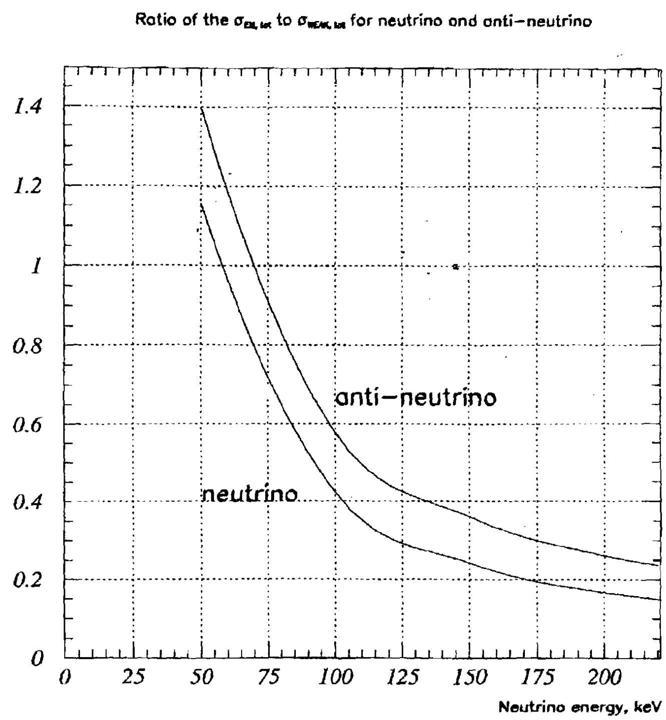
Ratio of the $\sigma_{EM,tot}$ to $\sigma_{WEAK,tot}$ for neutrino and anti-neutrino
1.4
1.2
1
0.8
0.6
0.4
0.2
0
0
25
50
75
100
125
150
175
200
Neutrino energy, keV
anti-neutrino
neutrino

Fig. 7

References

[1] M.B. Voloshin, M.I. Vysotsky, Preprint ITEP-1, (1986)
M.B. Voloshin et al., Sov.Phys.JETP **64**, 446, (1986),
G.K. Leontaris, K. Tamvakis, Phys. Lett. **B224**, 319, (1989),
P. Raychaudhuri, Mod. Phys. Lett. **A4**, 111-114, (1989),
C.S. Lim et al., Phys. Lett. **B243**, 389-395, (1990),
J. Pulido, Phys. Rept. **211**, 167-199, (1992),
R.N. Mohapatra, PP-90-177, 12, (1990),
J. Pulido Phys. Rev. **D48**, 1492-1505, (1993),
E.K. Akhmedov, Phys. Lett. **B298**, 391-396, (1993).

[2] S.I. Blinnikov and N.V. Dunina-Barkovskaya, Mon. Not. R. Astron. Soc. **266**, 289, (1994)

[3] M. Fukugita, S. Yazaki, Phys. Rev. D **36**, 3817, (1987)// G.G. Raffelt, Phys. Rev. Lett. **64**, 2856, (1990)

[4] V.N. Kornoukhov, Preprint, ITEP 26-96, (1996)
V.N. Kornoukhov, Preprint, ITEP 90-94, (1994)
W.C. Haxton, Phys.Rev. C **38**, 2474, (1988)

[5] M. Baldo-Ceolin et al., Preprint ITEP, 35-92, (1992)
A.B. Golubchikov et al., Sov.Nucl.Phys, **310**, 2126, (1994)
J. Bernabeu et al., Preprint, FTUV/94-22, IFIC/94-20 (1994)
J. Segura et al., Preprint, FTUV/94-34, (1994)
I.R. Barabanov et al., INFN-AE-95-24, (1995).

[6] S.A. Fayans et al., Phys. Lett. B, **291**, 1, (1992)
V.Yu. Dobretsov et al., Sov.Nucl.Phys, **55**, 2126, (1992)

[7] Yu.V. Gaponov et al., Sov.Nucl.Phys, **22**, 328, (1975)

[8] M.J Cooper, Rep.Prog. Phys., 48, (1985), 415

[9] G.V. Domogatski, D.K. Nadejin, Sov.Nucl.Phys, **12**, 1233, (1970)
L.B. Okun, *Leptons and Quarks*, "Nauka", (1990)

[10] P. Vogel and J. Engel, Phys.Rev., **D 39**, 3378, (1989).

[11] V.L. Morgunov, I.O. Pilugin, Preprint ITEP, 20-96, (1996) (in Russian).

[12] E. Clementi, C. Roetti, Atomic Data and Nucl. Data Tables 14, 177 (1974).

[13] A. Görling, M. Ernzerhof, Phys. Rew., **A 51**, (1995), 4501.

[14] H. Schmider, R.P. Sagar, V.H. Smith, Phys. Rew.,**A 49**, (1994), 4229.

[15] L.D. Landau, E.M. Lifshits, *Quantum Mechanics*, "Nauka", (1974).

В.Л.Моргунов и др.

Слабое и электромагнитное сечение рассеяния низкоэнергичных нейтрино на электронах атома.

Подписан к печати 07.06.96 Формат 60x90 I/I6 Офсетн.печ.
Усл.-печ.л.0,75. Уч.-изд.л.0,5 Тираж I00 экз. Заказ 28.
Индекс 3649

Отпечатано в ИТЭФ, II7259, Москва, Б.Черемушкинская, 25